Contents lists available at ScienceDirect

International Journal of Rock Mechanics and Mining Sciences

journal homepage: www.elsevier.com/locate/ijrmms

# On the stress dependency of sand production coefficient in hydro-dynamical sanding criteria

Panayiotis Kakonitis [a], Elias Gravanis [b,c], Ernestos N. Sarris [a,*]

[a] Department of Engineering, Oil and Gas Program, University of Nicosia, Nicosia, CY-1700, Cyprus
[b] Department of Civil Engineering and Geomatics, Cyprus University of Technology, Limassol, CY-3036, Cyprus
[c] Eratosthenes Centre of Excellence, Cyprus University of Technology, Limassol, Cyprus

ARTICLE INFO

*Keywords:*
Sand production
Sanding criterion
Surface erosion
Hydrodynamic models
Sand production coefficient
Degradation
Poroelastoplasticity
Hollow cylinder

ABSTRACT

Solids production is a complex physical process which is controlled by several factors including mechanical failure from in-situ stresses and hydrodynamic erosion from fluid flow. Hydrodynamic models for the prediction of sand production involve sanding criteria based on filtration theories. Such models contain a constitutive model parameter, the coefficient $\lambda$, with dimensions of inverse length which is calibrated by sand erosion tests, but its nature and its dependencies have not been clarified to date. The aim of this work is an attempt to refine the hydrodynamic models by investigating the dependence of the sand production coefficient $\lambda$ on the external stress conditions and on the plastic zone $\Lambda$ that is developed on hollow cylinders tests and propose an expression describing its importance in the sand production prediction modelling. The aim of the work is obtained through simulations with finite elements by utilizing the well-established Arbitrary Lagrangian-Eulerian (ALE) analysis considering the poro-mechanical coupling of the fluid-solid system for simulating hollow cylinder tests. Best fitting experimental data estimated values for the sand production coefficient for various values of external stress are obtained through back analysis. The dependence of $\lambda$ on the external stress turns out to be fairly smooth and a three-parameter model is proposed to describe that dependence: a scale parameter, an exponent, and a stress parameter defining the magnitude of stress at which erosion onset is predicted. It turns out that the stress parameter is associated with the minimum stress required for plastic yielding to occur, which was also estimated theoretically. This finding is in agreement with the physical assumption underlying the simulations that erosion onsets and progresses after the material reaches a critical plastic strain as a consequence of material plastic yielding. A power law model describing the dependence of $\lambda$ on the plastic zone depth is also proposed and discussed.

## 1. Introduction

Predicting the volume of solids produced (sand particles) from producing oil and gas wells has been one of the problems requiring solution in the context of hydrocarbons recovery. This is because of the aggressive production schedules the operators apply in the reservoirs, which in turn increase the stresses on the rock by applying higher drawdown pressure. The straining of the reservoir rock causes local failure at the wellbore walls thereby resulting in the production of solids along with hydrocarbon fluids. Most petroliferous rocks are sandstones therefore understanding the mechanics of the erosion process is very important because it costs to the producers multiple millions of dollars each year.[1] Few of the costly complications include perforations plugging, production liners or screens blinding, downhole equipment erosion by abrasion, wellbore stability issues which may result in catastrophic failures.[2–6]

The modelling of the physical problem of sand production is by no means a trivial process as it involves a strong coupling between the hydro-dynamical and mechanical processes which are associated with fluid flow, solids mobilization, fluid-rock interaction, and rock deformation. The phenomenology of the process, by field and experimental observations, is that the rock initially fails mechanically on the wellbore wall surface and then fluid flow erodes the mechanically failed rock flake by flake which eventually are flashed-out. When these flakes are removed from the wellbore surface, porosity is increased, and new discontinuities appear. The failure rate is further increased by the

* Corresponding author.
*E-mail addresses:* kakonitis.p@live.unic.ac.cy (P. Kakonitis), elias.gravanis@cut.ac.cy (E. Gravanis), sarris.e@unic.ac.cy (E.N. Sarris).

https://doi.org/10.1016/j.ijrmms.2023.105443
Received 12 February 2022; Received in revised form 8 January 2023; Accepted 30 May 2023

concentrated stress on the discontinuities. Computationally, the failure mechanism is understood as a two-step coupled process involving material failure (encoded in a yield criterion), and the mobilization and removal of particles by the hydrodynamic forces at work. Sand production, can be quantified by a volume of produced solids against time graph, exhibiting the physical response of the rock under given external stress and flow conditions.[7–12]

Papamichos et al., in (2001)[13] claimed, through laboratory experiments on hollow cylinder tests, that plastic yielding is the cause of micro-cracks, resulting from the application of external loads, which may serve as erosion starting points. However, this statement was challenged by other investigators by conducting experiments under true triaxial stress state on cubic samples which have shown that yielding of the material around the wellbore surface is not necessarily an indicator for on-setting sand production.[14]

Adopting the point of view that plastic yielding serves as erosion starting point, then the sand erosion problem can be treated numerically as a wellbore stability issue, however, predicting the sand production onset only.[15] On the other hand, several numerical models attempt to pseudo-couple fluid flow and mechanical failure of rock increasing the computational difficulty. However, such models suffer from the limitation that they do not capture the progressive damage of the rock which actually occurs (e.g. grain cohesion softening with simultaneous friction hardening).[8,16] Few earlier works relating plastic yielding to sand production in a producing well can be found in.[17,18] However, the proposition that sand onset and plastic yielding has proven to be conservative both experimentally and theoretically. To solve that issue, critical plastic strain criteria were adopted to predict sand onset numerically.[19]

A somewhat recent attempt was made in[9] where an erosion semi-analytical model was built upon the physics of the coupling between the poro-mechanical failure and the fluid flow. In that model, material softening is incorporated via Young modulus-softening and cohesion-softening. The model was validated with the experimental data of the volumetric sand production from hollow cylinder tests of.[13] Simulations based on this model was also performed in.[19,20]

The hydro-dynamical model of Vardoulakis et al. (1996)[7] involves the so-called sand production coefficient λ, which has dimensions of inverse length $[\lambda] = L^{-1}$. The sand production coefficient λ is a phenomenological coefficient appearing in the solids mass production equation which controls the rate of the erosion process. It can be envisioned as the strength of erosion because when it is constant its contribution to the erosion process is purely hydrodynamical. Also, the higher the coefficient the larger the sand production predicted. According to the seminal work presented in,[7] this coefficient was thought to be related to the spatial frequency of potential erosion starter points. These erosion starter points are linked with the solid skeleton of the porous medium and as such, its merit could be potentially associated with the grain size and minerology of the material. Furthermore, in their work[7] it was stated that this coefficient can be determined experimentally, and it should be kept in mind that due to the coupling between erosion process and rock weakening, λ is expected to be an increasing function of rock damage.[7,8] However, to the authors knowledge, a dedicated set of tests for determining the value and the properties of the sand production coefficient does not exist. Modelling-wise, the dependence of λ on the damage has been encoded by a plastic shear strain function.[3,5,9,13,21] The physical interpretation of modelling λ with a plastic shear strain function is that it captures the effect of the rock damage associated with the grain size and minerology of the material.

In this work, we constructed a coupled hydro-mechanical finite element model to overcome the difficulties in the listed references of this work by (i) coupling mechanical failure-fluid flow, (ii) predicting erosion onset and (iii) capturing progressive damage of the rock. The proposed model accounts all the above and simulates the sand production process in hollow cylinder tests. With the created finite element model we investigate numerically the effect of the stress magnitude on the sand production coefficient λ and put forward a simple mathematical expression describing that dependence. To this end, for on-setting the sand production we use the volumetric criterion via a user subroutine coded in Fortran, as it was proposed by[22] which involves the sand production coefficient. This provides the flexibility to modify the function of the sand production coefficient and predict the particles concentration that is produced through an Arbitrary Lagrangian-Eulerian (ALE) adaptive meshing technique, allowing for the mesh to move independently of the material and with respect to the original configuration of the mesh. By varying the value of λ, we find by trial and error a set of volumetric sand particle curves produced numerically which best describe the experimental volumetric curves of[13] for different stress magnitudes. This allows us to deduce an empirical mathematical relation for the dependence of the sand production coefficient on the external stress.

This paper is organized as follows: in section 2 the governing equations of the model are presented. Section 3 describes the finite element model while in section 4 the produced results are presented and critically evaluated. Finally, in section 5 we outline the main findings of this work.

## 2. Theoretical model of sand production

The governing equations describing sand production is not trivial and may be broken down into two physical processes. The first one is the poro-mechanical response of the rock sample and the second is the erosional response of the rock fabric. The poromechanical processes are described by the theory of poroelastoplasticity while the hydrodynamics is modeled by filtration theories.[7,9,13]

In our context, the rock formation is considered single-phase fluid-saturated assuming quasi-static state conditions for the rock deformation and fluid flow. Under quasi-static conditions, the governing equations for poro-mechanical response are as follows[13,15,23]:

$$\text{Equilibrium equations}: \sigma_{ij,j} = 0 \tag{1}$$

$$\text{Porous solid response}: d\sigma_{ij} = C^{ep}_{ijkl} d\varepsilon_{kl} + \alpha dp\delta_{ij} \tag{2}$$

$$\text{Fluid continuity}: q_{i,i} = 0 \tag{3}$$

$$\text{Darcy's law}: q_i = -\frac{k}{\mu} p_{,i} \tag{4}$$

where $\sigma_{ij}$ are the total stresses, $\varepsilon_{kl}$ are the shear strains, $p$ is the pressure in the fluid, $q_i$ is the fluid flux, $C^{ep}_{ijkl}$ is the tangent poroelastoplastic stiffness matrix, $\alpha$ is the Biot coefficient, $k$ is the permeability, $\mu$ is the fluid viscosity and $\delta_{ij}$ is the Kronecker delta.

For the erosional response, the governing equations are[7,13,22]:

$$\text{Solids continuity}: \frac{\dot{m}}{\rho_s} = \frac{\partial \varphi}{\partial t} \tag{5}$$

$$\text{Solids mass creation}: \frac{\dot{m}}{\rho_s} = \lambda(1-\varphi) q_i \tag{6}$$

$$\text{Kozeny} - \text{Carman}: k = k_0 \frac{\varphi^3}{(1-\varphi)^2} \tag{7}$$

where $\dot{m}$ expresses the erosion rate (solids mass rate per unit of volume), $\varphi$ is the porosity of the rock, $\rho_s$ is the rock density, $k_0$ is the Kozeny-Carman parameter that is related to the initial permeability and $k$ is the permeability. Eq (7) describes the strong variation of permeability with porosity.

Equation (6) is the constitutive equation for sand production mainly intended for oil wells. Simulations using (6) imply that sand erosion for the case of gas will produce significant amounts of sand due to low viscosity and thus high flow rates. At this point it is considered

important to mention that this has not been justified by experiments. The physical content of this model is that the erosion rate is proportional to the fluid flux, and also it depends on the remaining mass as implied by the factor $(1-\varphi)$. These are the simplest plausible assumptions for a constitutive erosion equation as put forward by[7] based on filtration theories. The sand production coefficient $\lambda$ is the proportionality constant of the constitutive law (constitutive parameter), with dimensions of inverse length and can be determined experimentally by sand erosion tests. For some researchers, it is considered as an empirical constant/function which requires special treatment.[8,9,13]

Experimental work implies that erosion onsets when the stress magnitude exceeds a certain threshold depending also on the fluid flow, for any given rock type.[13,15] When this threshold is reached then the material shows a softening behavior.[9,13,19] Assuming that the sand production coefficient is a function of the plastic strain the softening behavior is encoded in the constitutive equation.[5,13,19,21] Associating erosion with plasticity, solved an important weakness of the original formulation of the constitutive equation,[7] which implied that significant erosion from the bulk of the material, contrary to the experimentally observed erosion localized on the surface. The sand production coefficient as a function of the shear strains is given by[5,13,21]:

$$\lambda\left(\varepsilon^{pl}\right)=\begin{cases}0 & if \quad \varepsilon^{pl}\le\varepsilon^{pl}_{thr}\\ \lambda_1 & if \quad \varepsilon^{pl}_{thr}\le\varepsilon^{pl}\le\left(\varepsilon^{pl}_{peak}+\lambda_2/\lambda_1\right)\\ \lambda_2 & if \quad \varepsilon^{pl}\ge\left(\varepsilon^{pl}_{peak}+\lambda_2/\lambda_1\right)\end{cases} \tag{8}$$

where $\varepsilon^{pl}$ is the plastic shear strain, $\varepsilon^{pl}_{thr}$ is the plastic shear strain value at which erosion is turned on, $\varepsilon^{pl}_{peak}$ is the plastic shear strain at maximum sand production coefficient, $\lambda_1, \lambda_2$ are calibration constants to be determined through calibrations[5,13,21] as stated in the literature. To the authors' knowledge, no tests exist providing values for the constants in model given in eq. (8), neither a verification of its form.

The aim of the present work is to provide certain insights in the nature of the sand production coefficient and in particular its dependence on the external conditions applied on the material. Equation (8) implies that sanding onsets gradually when the plastic strain exceeds a certain value, reaching a plateau beyond the limiting value of the plastic strain. In this work we adopt a simplified version of the model in Eq. (8), neglecting the gradual transition to the plateau, which does not have a solid physical justification and in order to keep the parameters of this model to a minimum. We propose that the sand production coefficient may simplify as[19]:

$$\lambda\left(\varepsilon^{pl}\right)=\begin{cases}0 & if \quad \varepsilon^{pl}\le\varepsilon^{pl}_{thr}\\ \lambda_2 & if \quad \varepsilon^{pl}\ge\varepsilon^{pl}_{thr}\end{cases} \tag{9}$$

The plot of both functions (equations (8) and (9)) is shown in Fig. (1).

Expression (9) allows for a delay in on-setting the erosion phenomenon as plastic deformation develop and advance. The simplicity of the model (9) is consistent with the fact that the hollow cylinder rock sample are very small, hence we expect that any transient phenomena at the problem at hand will be minimal to influence the overall solution. At larger scale models such phenomena may be important although no detailed phenomenological analysis exists. Both, the time delay and calibration constant $\lambda_2$ are fitted so that the numerically produced sand production curve to compare quite well with the experimental.[13] The following section presents the finite element model that was created for the purposes of this investigation.

## 3. Finite element model

The finite element model simulates the hollow cylinder test of Papamichos et al. (2001) in[13] for a 2-D model with an inner radius $r_w = 0.01$ m, an external radius $r_e = 0.1$ m and cylinder height $H = 0.2$ m under plane strain conditions. At this point it is assumed that the plane strain assumption used for the modeling will not influence quantitatively the results. The geometry of the rock samples allows for quarter symmetry. The model is sufficiently meshed around the cavity in order to be able to resolve any small variations on the inner face of the specimens caused by erosion. The finely meshed region extends 0.02 m from the initial inner radius $r_w$. The model dimensions and the local region mesh refinement exclude any boundary effects (i.e the numerically eroded surface will remain close to the inner hole rather than reaching the external boundary). The geometry and the detailed finite element model is shown in Fig. (2): $\sigma_h$ is the external radial stress and $\Lambda$ is the length of the induced plastic zone.

The finite element model was created with the commercial software.[24] The model is fully coupled, hence the deformations and the pore pressure degrees of freedom are the unknown variables determined by the simulations. The finite element considered is the widely used CPE4P which is a 4-node (with 23162 nodes in total) bilinear displacement and pore pressure quadrilateral element (with 23184 elements in total). With this problem size it is ensured that the amount of sand produced will be accurately captured since the area available for erosion localizes in a short regime near the hole dictated by the experimental hollow cylinder tests (see Table 1).

According to the physics of the model described in section 2, the application of radial external stress causes stress concentration at the inner surface of the hollow cylinder inducing local plastic strains which allows the onset and advancement of the erosion process. The simulation proceeds in two steps: (A) an initial equilibrium step which allows the material to respond to the external load, and (B) the dynamic step, in which flow rate is turned on, poroplastic deformations develop creating a plastic zone of depth $\Lambda$ and the erosion process onsets and progresses. Both solution steps operate under symmetry conditions $d_x = 0$ at the vertical axis, $d_y = 0$ at the horizontal axis. The shear stresses at the symmetry planes are considered to be zero. On the internal boundary of the hollow cylinder, we applied zero radial internal pressure and zero fluid pressure. On the external boundary, we applied a set of different

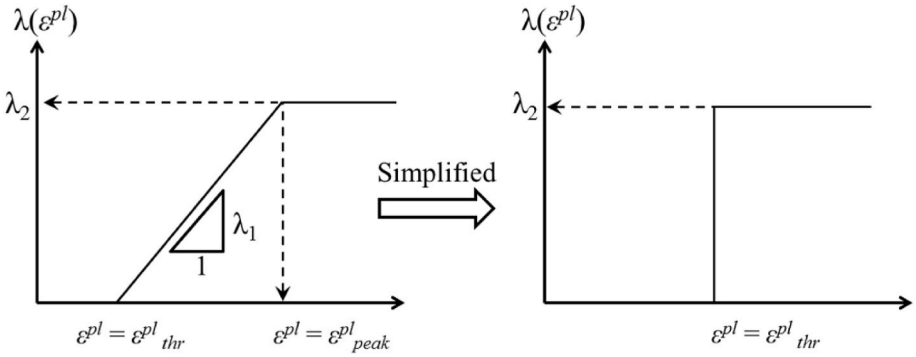


**Fig. 1.** Detailed description of the sand production coefficient behavior (eq. (8)) and (eq. (9)) used in the simulations.

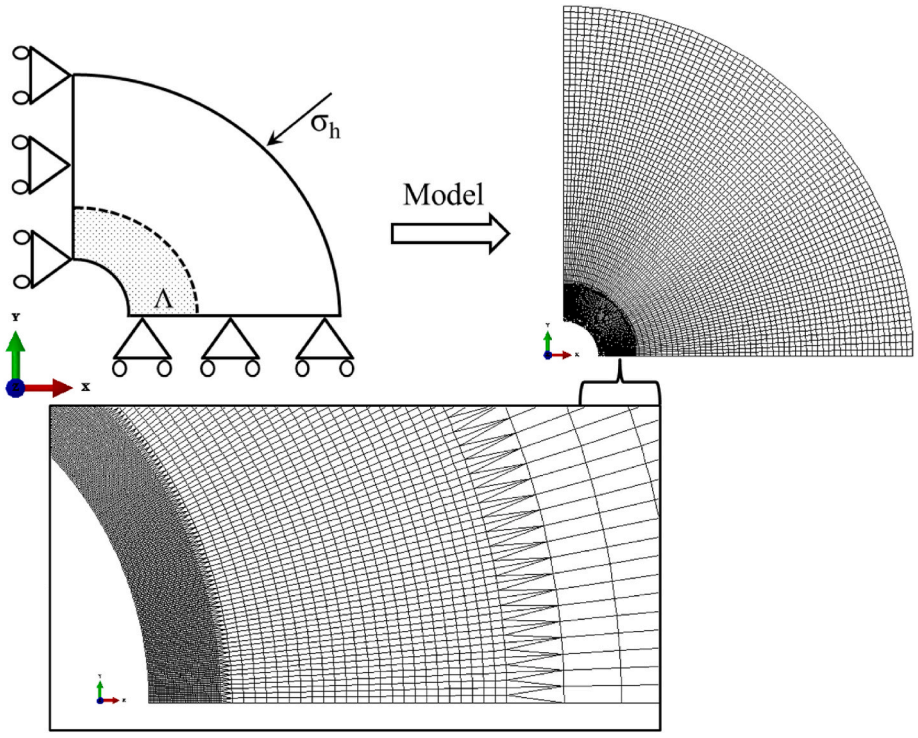


**Fig. 2.** From geometry to the application of boundary conditions and the resulting finite element mesh with a detail depiction of the very fine elements in the erosion region.

**Table 1**
Input parameters used for the simulations.

| Variable | Value |
|---|---|
| **Geometric Properties** | |
| Hollow cylinder internal radius, $r_{in}$ [m] | 0.01 |
| Hollow cylinder external radius, $r_{out}$ [m] | 0.1 |
| Cylinder height, $H$ [m] | 0.2 |
| **Porous rock and fluid properties** | |
| Young modulus, $E$ [MPa] | 6750 |
| Poisson ratio, $\nu$ [−] | 0.19 |
| Cohesion, $C$ [MPa] | 3.7 |
| Friction angle, $\Phi$ [$^0$] | 37.4 |
| Initial porosity, $\varphi_0$ [-] | 0.3 |
| Initial rock permeability, $k$ [md] | 500 |
| Solids density, $\rho_{solid}$ [kg/m$^3$] | 2640 |
| Kozeny-Carman parameter, $k_o$ [m$^2$] | 8.956E-12 |
| Dynamic viscosity, $\mu$ [MPa·s] | 5.0E-9 |

external radial stresses $\sigma_h = \{7.5, 8, 9, 10, 11\}$ MPa while also considering a constant external pressure $P_{ext} = 0.15$ MPa throughout the simulations. For each stress level, erosion was initiated and allowed to produce sand particles for 8000sec. With the aforementioned boundary conditions the initial flow rate $Q$ that passes through the hollow cylinder is given by:

$$\text{Flow rate}: Q = 2\pi k_0 H \frac{P_{ext}}{\ln\left(\frac{r_e}{r_w}\right)} \tag{10}$$

Assuming a Kozeny-Carman coefficient $k_0 = 8.956\text{E-}12$ m$^2$ expression (10) yields Q = 0.5 L per min.

The simulation of sand production process leads to significant deformation of the material, around the inner hole of the hollow cylinder being modeled. The deformation is captured accurately by refining with finite elements the regime which erosion is expected to be take place. For this reason, high quality and sufficient meshing is important in the modelling. In conventional, Lagrangian based finite element analysis, the element nodes are connected to the material. Any deformation resulting from changes of the material will reflect on the finite element mesh because the material boundary coincides with the element boundary. This procedure will create moving surfaces and with the application of boundary conditions, excessive finite element distortion which will result in large deformations condemning the method inappropriate for simulating the sand production process. On the other hand, the Eulerian based finite element analysis, allows for material changes to take place while the element nodes stay fixed in space. As it is evident, with the Eulerian analysis mesh distortion is not possible and the application of boundary conditions becomes a major challenge as the material flow must be tracked down as a moving surface. The Arbitrary Lagrangian-Eulerian (ALE) finite element analysis is an adaptive meshing technique that combines the advantages of the Lagrangian and the Eulerian analyses to simulate moving boundary/surface problems. The advantage of ALE method is that mesh deformation can behave independently from material changes making it elegant for simulating the erosion process while preserving high quality of finite element mesh throughout the simulation, even when either excessive deformation or loss of materials occurs. For this reason, the ALE methodology was considered the most appropriate for the purposes of this work. The ALE adaptive meshing and adaptive constraints are available in Abaqus. A detailed analysis on the ALE adaptive meshing can be found in.[5,21] Physically, the erosion process results in progressive removal of material from the free inner surface of the rock sample. Modelling-wise the process is described by updating the boundary conditions on the continuously created new surface emerging from the removal of material once the volumetric criterion is met.

The rock samples are modeled as sandstones obeying a Mohr-Coulomb yield surface. For the elastic component of the model, the Young modulus and the Poisson ratio are assumed constant throughout the simulations (i.e. Young Modulus-softening was not included in the modelling). For the plastic part, the Mohr-Coulomb criterion is described with the following properties: cohesion, friction angle and dilation angle.

Here, we take into account the cohesion softening of the rock

through the erosion process. The cohesion-softening in this model is encoded by a plastic strain dependency of the cohesion parameter given by the linear softening following the equation $C = 3.7 - 50\,\varepsilon^{pl}$ [MPa]. At this point we assume that the cohesion of the material due to the softening behaviour will not reach zero at failure. This assumption is justified by experimental investigations.[25] For the relevant range of values of the plastic strain the dependence of the cohesion on $\varepsilon^{pl}$ is shown in Fig. 3. The simplicity of this model is discussed below.

The porous properties of the rock are described by the dynamically evolving porosity and permeability which arise as part of the solution, starting from a uniform value of porosity. The input parameters for the simulations include the geometry, the porous rock and permeating fluid properties and are summarized in table (1). All the physical parameters are taken from[13] The iterative numerical solution of the non-linear system of equations (section 2) is done via the Newton-Raphson method. The continuity equations are integrated in time via a back-ward Euler scheme and all variables are updated at the end of each increment.

Finally, we acknowledge the following modelling and simulation assumptions: (A) The adopted hydrodynamic model describing the volumetric sand production (eq. (6)) associates the erosion process with material yielding (plasticity) as a function of the external radial stress applied at the hollow cylinder boundary. This assumption creates maximum output of material yielding (e.g. worst case scenario) for a given external radial stress magnitude. This assumption yields sand production prediction rather conservatively both experimentally and theoretically. We acknowledge that critical plastic strain criteria are also available to predict sand production numerically, but the intention of this work is an attempt to create an understanding on the volumetric sand production coefficient λ, and its dependencies with stress magnitude and plastic zone development using as few parameters as possible. (B) We assume that the ALE formulation in the proposed finite element model predicts sufficiently and accurately erosion onset and sand production. The assumptions outlined above amount to a convenient approximation allowing to propose our model. To the authors knowledge, no complete physical understanding of sand production coefficient λ is known, therefore reducing the parameters influencing the problem (e.g. equation (9)) is a rather good way to proceed with the investigation. Under these conditions the model could be potentially applicable to more complex stress states (e.g. 2d or 3d anisotropic stress fields) and at any scale from experimental to field-scale.

## 4. Analysis of simulation results

Fig. 4 shows the dependency of the initial value of the plastic zone depth Λ on the external radial stress. The blue circle markers correspond to the studied values of the stress $\sigma_h = 7.5, 8, 9, 10, 11$ MPa while the single red square marker corresponds to 7.46 MPa radial stress just to initiate plastic yielding of the material. These results are obtained numerically from the simulations with Abaqus after balancing the application of the external radial stress steps of ($\sigma_h = 7.5, 8, 9, 10, 11$ MPa) with material plastic yielding just before the erosion onsets. These results are in complete agreement with the solution of the poroelasto-plastic equations presented in Gravanis et al. (2015) [9]and are shown in orange cross markers.

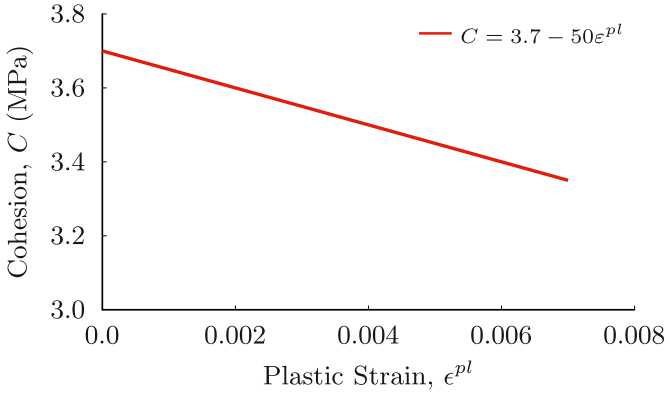


**Fig. 3.** Representation of the linear cohesion softening as a function of plastic strains.

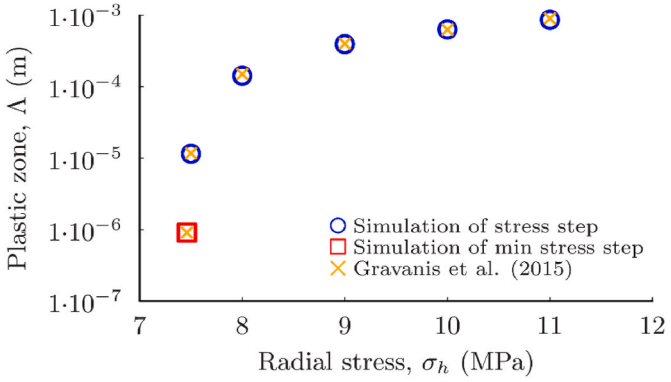


**Fig. 4.** The initial plastic zone dependency on the externally applied radial stress.

The results show that the lowest value of the stress considered experimentally (7.5 MPa) causes significantly smaller plastic zone than the other values. Also, below that value the size of the plastic zone decreases quickly and vanishes at a value somewhat less than 7.46 MPa. This behavior (plastic yielding) of the material is strongly related to each behavior regarding the erosion process, as it will be discussed below.

Fig. 5, presents the sand production curves as derived from the finite element model, for all values of $\sigma_h$ and compared with the experiments of Papamichos et al. (2001)[13] and the mathematical results of Gravanis et al. (2015).[9] The experiments are represented with circle markers, the mathematical results with dashed lines and the simulation with continuous lines. The simulations were run for 8000 s i.e. 2.22 h of sand production. One should bear in mind that the sand production coefficient $\lambda$ in the constitutive equation is turned on when plastic equivalent strains for the Mohr-Coulomb yield criterion exceed a certain value ($\varepsilon^{pl}_{thr}$), as shown in Fig. 4, beyond which $\lambda$ remains constant. This creates a certain "delay" in the erosion onset. With $\lambda$ constant, that implies that the simulated eroded mass curves do not contain the transient regime of the experimental curves which is a result of the way the experiment was performed (stress was increased stepwise gradually from 3 MPa to failure, above 11 MPa). By trial and error, we determine after a number of simulations the value of the parameters $\varepsilon^{pl}_{thr}$ and $\lambda_2$ for each value of the external stress considered in the experiments of,[13] so that the simulated eroded mass curves best fit the experimental data. It is important to mention that the starting time of erosion should get shorter as the stress values go larger which is explained by the transition time of the experiments. In the presented results this is not captured because the erosion starting time is the result from trials so as to find the optimum $\varepsilon^{pl}_{thr}$ and $\lambda_2$ which do not appear to have this trend. Also, for completeness we include the theoretical sand production curves of,[9] although the latter are obtained with a different model for the sand production coefficient. Additionally, from the point of view of the material, an elasto-plastic behavior with hardening could be used to possibly reduce the discrepancy in the transient regime between the experiments and the simulations. However, this will result in increasing the number of parameters influencing the estimate of $\lambda_2$ while our intention here was to produce a hard estimate for the sand production coefficient. This is in line with our choice to keep the input parameters at a minimum which we also adopted in the hydrodynamic model.

From the analysis it is shown that the numerical model captures

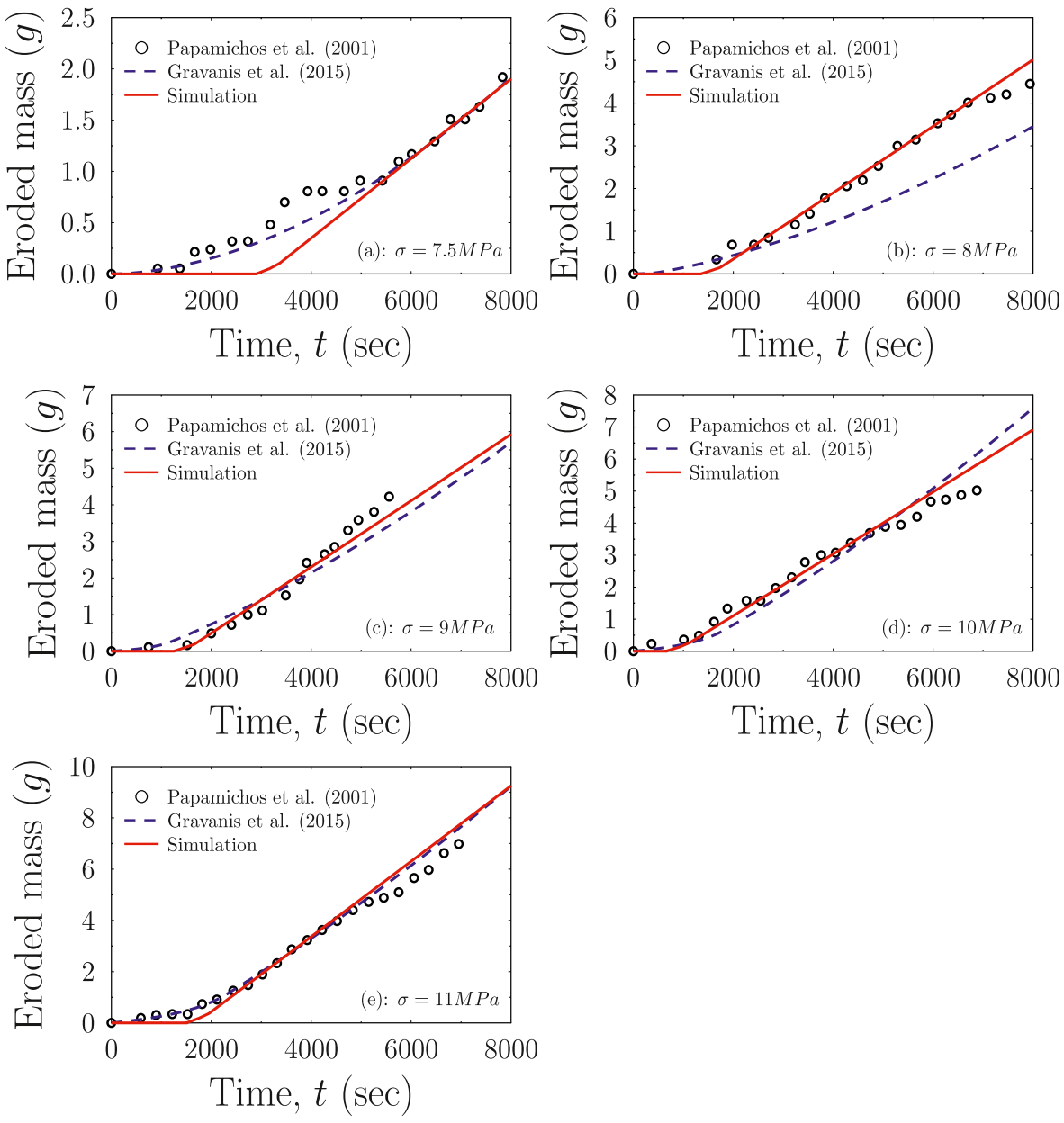


**Fig. 5.** Comparison of sand production curves between experimental (Papamichos et al., 2001), mathematical (Gravanis et al., 2015) and numerical for the various external radial stresses $\sigma_h = \{7.5, 8, 9, 10, 11\}$ MPa considered.

within reasonable accuracy the experimental for all the values of radial stresses considered. One should observe that, essentially by the constancy of the sand production coefficient, the eroded mass rate is nearly constant in the simulations, however, one should note that at early times a transient regime exists which is associated with the middle term of equation (8) that we have reduced in the modelling via a Fortran subroutine. This fact together with the issue of the transient parts of the experimental curves creates differences between them and the simulations, which are quite visible in the 7.5 MPa case. After a certain time of sand production, the surface area of the hollow cylinder enlarges which reduces the frictional forces between the solid particles. This has the direct result of reducing the sand production as it is seen in the experimental curves under external level $\sigma_h = 7.5$, 8, and 10 MPa. This late times effect (friction softening) cannot be captured by the current model and will be the focus of future work. Furthermore, in Fig. 5 there appears to be a better agreement between the simulations and other results at higher stresses. The reason for this observation is that at low stress magnitudes the erosion process evolves slowly thereby creating prolonged transient regimes until stabilized sand production can be observed. For higher stress magnitudes, the erosion process evolves faster suppressing the transient regime reaching earlier stabilized sand production.

Fig. 6 shows the tangential and radial stresses as a function of distance for the case of 11 MPa external stress for the simulations (dashed-red) and the mathematical model of Gravanis et al. (2015)[9] (continuous-blue), for early times and late times respectively. These curves show the effect of softening on the stress fields as time evolves. As expected, as time progresses the tangential stresses drop at the inner surface of the hollow cylinders causing also the lowering of the peak value at the boundary of the plastic zone. Furthermore, as erosion progresses, it also shown that the peak values move away from the hollow cylinder axis thereby showing the progressive evolution of the erosion process. The radial stress field configuration moves also away from the cylinder axis as more material is eroded away. One may note that although the

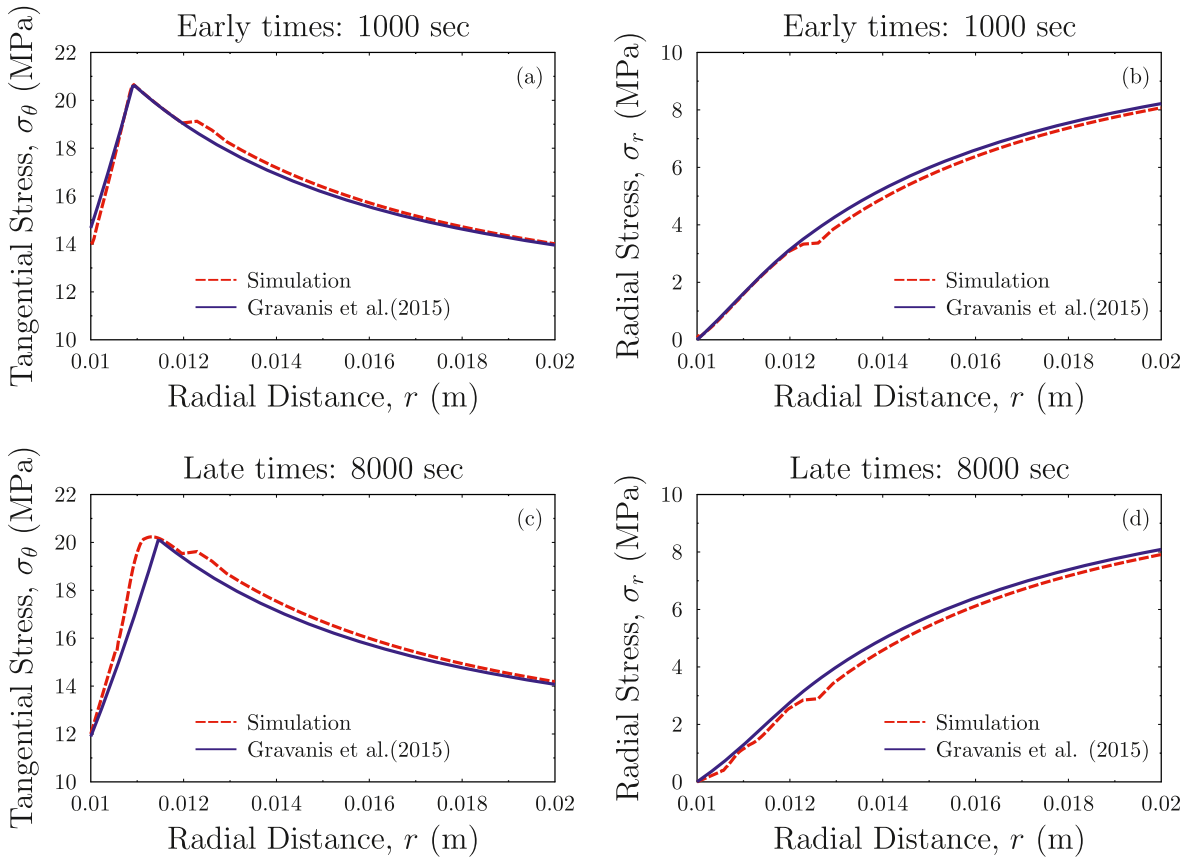


**Fig. 6.** Comparison between the simulations and the solution of Gravanis et al. (2015). (a) Tangential stresses and (b) radial stresses for early times 1000 s (0.27 h), (c) tangential stresses and (d) radial stresses for late times 8000 s (2.22 h).

mathematical model has a completely different form of softening (cohesion depends on the evolving porosity), the rough effect of cohesion softening on the stress fields is nearly similar, for nearly the same sand production.

The analytical model is constructed entirely on a different methodology as compared with the proposed finite element model. The analytical model of Gravanis et al. (2015)[9] is expected to behave better because it considers the degradation of both the cohesion and the young modulus of the material under consideration and the erosion coefficient is given by a 3-parameter model which allows for flexibility in the transient regime. However, in that work it was shown that the degradation of the young modulus does not yield any significant results and the contribution of the erosion strength stems from the material cohesion and the erosion coefficient which is very elegant for finite element modelling. The proposed finite element model considers the cohesion softening as a function of the plastic strain level and with the reduced erosion coefficient function (eq. (9)). It is important to note that the transient regime was reduced to simplify the parameters affecting the problem to a minimum. Despite their differences, the end-result of sand production prediction compares fairly well. However, due to the simplification of eq. (9), we acknowledge the discrepancies observed the transient part of the sand production curves. Another strength of the proposed model is shown in Fig. 6, where the tangential and the radial stresses compare quite well for early and late times. Since the finite element model compares with experimental data and an analytical solution, it can be extended to include more complex stress states and in more complex geometries other than the hollow cylinder tests that it was constructed for, where the analytical solution cannot be applied.

The previous analysis allows us to study the dependence of the sand production coefficient, determined by back analysis, on the magnitude of the external stress. Such a model fills an important gap in our current understanding of the hydrodynamic model given in eq. (6) describing solids mass production. We best fit the values of sand production coefficient by back analysis with a suitable power law function, given in eq. (11):

$$\text{Erosion coefficient}: \lambda_2 = \lambda_{2,0}\left(\frac{\sigma - \sigma_{\min}}{\sigma_{\min}}\right)^n \tag{11}$$

where $\lambda_{2,0}$ is a scale for the sand production coefficient (units inverse length), $\sigma$ is the stress level at the external boundary (i.e. in the model is $\sigma_h$) while in general $\sigma$ denotes the minimum insitu stress. $\sigma_{\min}$ is the least stress level to cause plastic yielding of the rock and $n$ is an exponent. We find the values: $\sigma_{\min} = 7.49$ MPa, $n = 0.1641$, $\lambda_{2,0} = 0.0912\, m^{-1}$. The usefulness of the proposed model (equation (11)) is that the erosion coefficient $\lambda$ which appears in the constitutive law (equation (6)) depends on a number of factors and parameters of the erosion process. Here, we merely investigate the dependency on the external stress field. Furthermore, we show that with this model $\lambda_{2,0}$ will be the same for all external stress levels, $\sigma_{\min}$ can be predicted analytically (see appendix) and $n$ is an exponent that can be obtained relatively easy as a fitting parameter. With this way we reduce the number of unknowns to determine the value of the erosion coefficient $\lambda$, which is usually treated as a complex 3-paremeter function with a number of dependencies. One may criticize that we still have to determine $\lambda_{2,0}$ which has the same dimensions [1/m]. Indeed, but in the proposed model $\lambda_{2,0}$ will be constant for all stress levels and will not vary as the stress field undergoes changes. Therefore, the model predicts the erosion coefficient $\lambda$ as a function of external stress only which is far simpler to obtain than the 3-parameter function. At this point it is important to note that we do not claim that the erosion coefficient $\lambda$ depends only on the external stress level. Other dependencies may exist (e.g. fluid flux). It also worth to note that the proposed empirical expression (11) was deduced from the

hollow cylinder test, with all its simplifications, model described by equation (11) has some general features that may be applicable to real field application.

Fig. 7 presents the sand production coefficient $\lambda_2$ as a function of the radial external stresses used to produce the numerical sand production curves of Fig. 5. The estimated sand production coefficient $\lambda_2$ is shown with circle marker. As mentioned above, the hydromechanical model employed in this work is based on the assumption that the onset of the erosion is related with critical plastic strain criterion following plastic yielding. In Fig. 4 we presented that the yielded zone for this specific material occur when the external stress exceeds a threshold which is just below the 7.5 MPa (in 7.46 MPa the plastic zone depth is 1 μm).

This is verified by the fitted value for the $\sigma_{\min}$ parameter of the power law model of Eq. (11) which indeed turns out to be just below 7.5 MPa. We should emphasize that this result follows solely from the trend of the $\lambda_2$ dependence on the external stress. Therefore, the $\sigma_{\min}$ parameter may be actually estimated theoretically, from the static poroelastoplastic solutions, see e.g.,[9] looking for the (maximum) value of the external stress that does not cause any plastic yielding. In fact, neglecting the effect of pressure one may derive an analytical expression (see Appendix) for the $\sigma_{\min}$ parameter, given by:

$$\sigma_{\min} = \left(1 - \frac{r_{\text{in}}^2}{r_{\text{out}}^2}\right) C \tan\left(\frac{\pi}{4} + \frac{\Phi}{2}\right) \tag{12}$$

For the specific material the conditions of the present problem we find the estimate to be $\sigma_{\min} = 7.41$ MPa which is 1% lower than the estimated value, that is, it is decently close to the best fit result of 7.49 MPa. In fact, taking $r_{\text{out}}$ to be large, this expression gives $\sigma_{\min} = 7.49$ MPa.

From the analysis performed, we see a physical connection between the sand erosion coefficient $\lambda_2$ and the plastic zone depth $\Lambda$. From the simulations, we have showed that the erosion coefficient $\lambda_2$ is influenced by the external stress level $\sigma_{\text{h}}$ but also affects the plastic zone depth. We propose another model describing the dependence of the sand production coefficient on the depth of the plastic zone, $\Lambda$, which as opposed in the model of eq. (11) encodes not only the properties for the material and the external stress but also the effect of the pressure drawdown as well. Mathematically, the model is given by:

$$\text{Erosion coefficient} : \lambda_2 = \beta \Lambda^{\gamma} \tag{13}$$

where $\beta$ is a dimensionful proportionality constant and $\gamma$ is an exponent. By best fitting to the values $\lambda_2$ estimated by back analysis we find $\beta = 0.4592$ and $\gamma = 0.2379$, where $\lambda_2$ and $\Lambda$ are understood in meters. Fig. 8 presents the model curve in continuous line and the estimated $\lambda_2$ in circle markers.

It is important to note how the plastic zone $\Lambda$ and their shape was determined. As discussed in the finite element model section, plastic yielding follows the Mohr-Coulomb criterion. The plastic zones are developed as a function of the stress level and continue to develop and evolve as material erodes away. The calculation of the plastic equivalent strains for the Mohr-Coulomb criterion are given by[24]:

$$\varepsilon^{pl} = \int \frac{1}{C} \sigma : d\varepsilon^{pl} \tag{14}$$

where $\varepsilon^{pl}$ are the plastic strain increments, $\sigma$ is the stress change in the material and $C$ is the material cohesion. Because the model is constructed as a hollow cylinder (see Fig. 2), the external stress boundary condition is uniformly applied in the radial direction which allows for a symmetrical plastic zone development. This geometric simplification allows for sand particles to be produced symmetrically from the cylinders' inner surface forming a cylindrical erosional surface. Fig. 9 shows the plastic zone development (eq. (14)) around the inner cavity of the hollow cylinder. Starting from the inner surface, the material than has eroded away is shown as a grey color region depicting that the eroded surface has progressed from its initial location. As the erosion process evolves, more material is made available for plastic yielding and in turn to erode. The material participating in plastic yielding, is the colormap region. Finally, the intact material that has not yielded is shown as the region with blue color. Thus, due to the symmetrical geometry and the radial boundary condition, the plastic zone shape can be easily determined. The simulation time for Fig. 9 is 8000 s or 2.22 h. It is important to note that for different geometries and stress state conditions, the erosional surface and the plastic zone shape determination will not be symmetrical. In such cases, the final eroded shape and plastic zone shape will be a natural outcome of the ALE solution ensuring actual erosional shape, plastic zone shape and numerical stability.

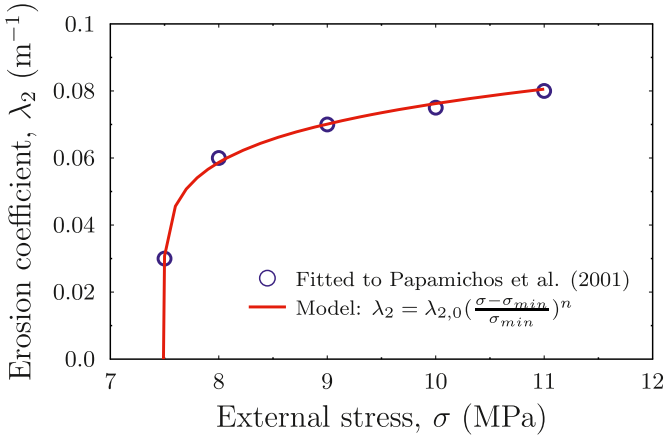


**Fig. 7.** The proposed expression to describe the dependence of coefficient $\lambda_2$ on external stress.

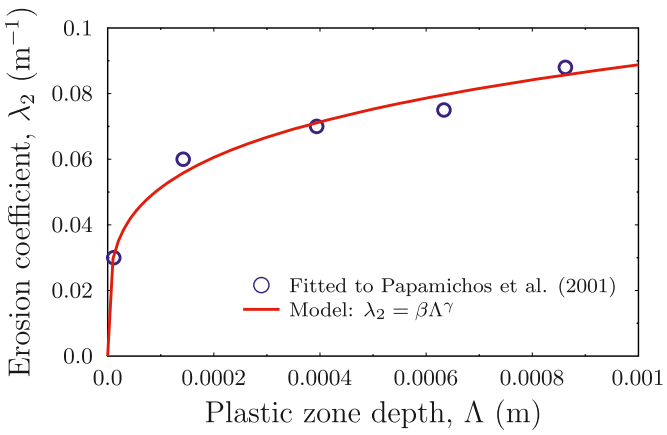


**Fig. 8.** The proposed expression to describe the dependence of coefficient $\lambda_2$ on plastic zone depth $\Lambda$

## 5. Conclusions

In this work, we revisited the problem of sand production in hollow cylinder tests in the context of the hydrodynamic modelling of the erosion process with the aim to provide the -currently inexistent- empirical relations for the sand production coefficient of those models as a function of the external conditions. Such relations may be anticipated on the basis of the physical assumptions of the hydrodynamic models of erosion which associate the erosion process with the effect of plasticity, as the latter is a result of the external stress.

To this end, we deduce empirical values for the sand production coefficient $\lambda_2$ by best fitting the experimental data of[12] with numerical simulations. The results show that $\lambda_2$ does indeed have a fairly smooth dependence on the external conditions. We propose two models to describe that dependence. The first one postulates $\lambda_2$ as a function of the

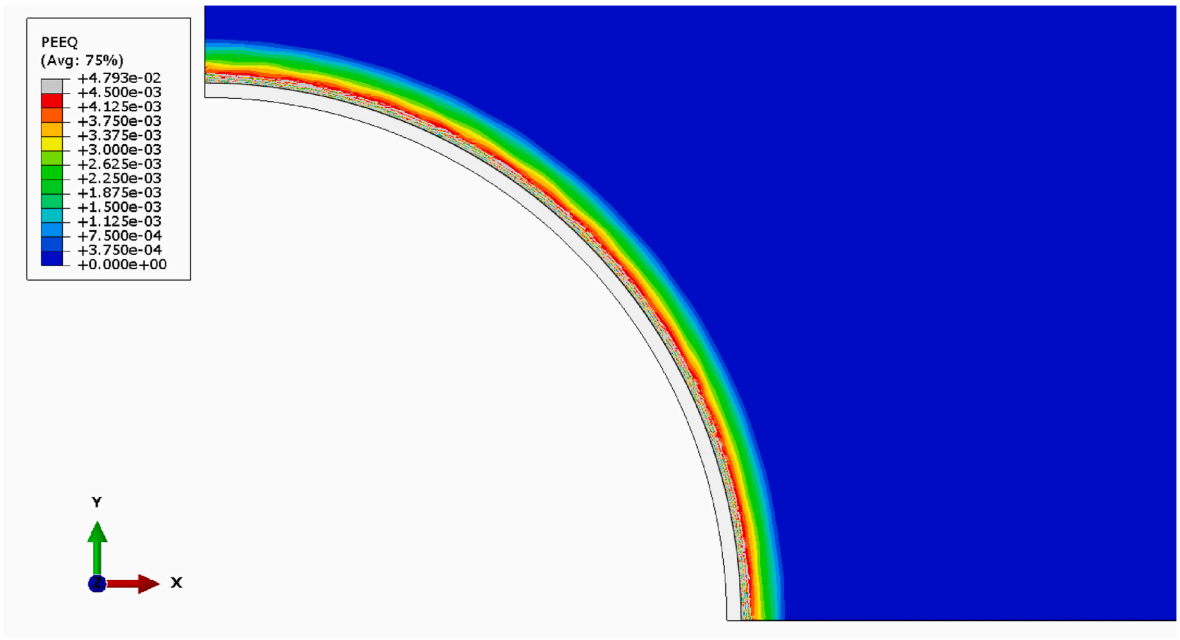


**Fig. 9.** Numerical solution for the equivalent plastic strains showing the eroded surface, the associated development of plastic zone $\Lambda$, and the shape of the plastic zone during evolution. Simulation time is 8000 s (2.22 h).

external stress and involves three parameters: a scale parameter, an exponent, and a stress value where $\lambda_2$ vanishes. It turns out that the latter parameter value is very close to the minimum external stress required for creation of plastic yielding. This finding, elaborates further the assumed association of the erosion process to plasticity. One may note, that the minimum stress for plastic yielding can be estimated theoretically and we provide the relevant result, thereby essentially eliminating one of the three parameters of the model. The second model we propose relates $\lambda_2$ with the plastic zone depth through a power law expression. The possible relevance of this model lies in the fact that the plastic zone depth includes the effect of pressure drawdown (although this effect is somewhat small in the case under consideration).

The proposals made in this work aim at refining the hydrodynamic erosion models in the direction of clarifying the nature of the purely phenomenological coefficient $\lambda_2$. In order to establish the range of validity of the proposed models, especially the stress dependent one, in particular the possible universality or the dependencies of the scale parameter and the exponent, further and detailed comparisons with experimental data is required. This is left for future contributions.

The proposed approach, used for the simulations can be considered a quite useful tool for characterization of soils, sediments, or any geological media in terms of their erosivity. Furthermore, the prediction of the volumetric erosion law parameters (e.g. $\lambda$) can be used in turn in predictive modelling. This also highlights its importance for simulating industrially related applications as a decision-making tool useful in well completions and perforation strategy management.

## Declaration of competing interest

The authors declare that they have no known competing financial interests or personal relationships that could have appeared to influence the work reported in this paper.

## Data availability

No data was used for the research described in the article.

## Appendix

We use the results of Gravanis et al. (2015) to derive eq. (12). Neglecting the effect of pressure, the stress field solution on the elastic side, i.e. $r > r_{\text{in}}+\Lambda$, is

$$\sigma_r = \sigma_{\text{out}} + C_2\left[\frac{1}{r_{\text{out}}^2} - \frac{1}{r^2}\right], \sigma_\theta = \sigma_{\text{out}} + C_2\left[\frac{1}{r_{\text{out}}^2} + \frac{1}{r^2}\right] \tag{A.1}$$

where $C_2$ is an integration constant to be determined by the continuity conditions across the plastic zone boundary, $\sigma_{\text{out}}$ is the external stress on the outer boundary of the rock sample, $r_{\text{out}}$ is the outer radius, and $r_{\text{in}}$ is the inner radius. The fields $\sigma_r$ and $\sigma_\theta$ are the radial and tangential stresses, respectively.

In the plastic zone side, i.e. $r < r_{\text{in}}+\Lambda$, the stress field is given by

$$\sigma_r = \sigma_{\text{in}}\frac{r^{K-1}}{r_{\text{in}}^{K-1}} - \frac{S_0}{K-1}\left[1 - \frac{r^{K-1}}{r_{\text{in}}^{K-1}}\right], \sigma_\theta = S_0 + K\sigma_r \tag{A.2}$$

where $\sigma_{\text{in}}$ is the inner radius stress, and

$$K = \tan^2\left(\frac{\pi}{4}+\frac{\Phi}{2}\right), S_0 = 2C\sqrt{K} \tag{A.3}$$

where $C$ is material cohesion [MPa], $\Phi$ is the material friction angle [$^0$], $S_0$ is the uniaxial compressive strength [MPa]. The continuity condition across the plastic zone boundary reads

$$\sigma_{r\ \mathrm{elastic}}(r_{\mathrm{in}}+\Lambda) = \sigma_{r\ \mathrm{plastic}}(r_{\mathrm{in}}+\Lambda), \sigma_{\theta\ \mathrm{elastic}}(r_{\mathrm{in}}+\Lambda) = \sigma_{\theta\ \mathrm{plastic}}(r_{\mathrm{in}}+\Lambda) \tag{A.4}$$

The first condition provides a value for the integration constant $C_2$. Setting the plastic zone depth $\Lambda = 0$, and considering the pertinent case $\sigma_{\mathrm{in}} = 0$, one straightforwardly finds

$$\sigma_{\mathrm{out}} = \left(1-\frac{r_{\mathrm{in}}^2}{r_{\mathrm{out}}^2}\right) C \tan\left(\frac{\pi}{4}+\frac{\Phi}{2}\right) \tag{A.5}$$

which we identify as an estimate for the $\sigma_{\mathrm{min}}$ parameter of the model in eq. (11).

## References


1 Mahmud HB, Leong VH, Lestariono Y. Sand production: a smart control framework for risk mitigation. *Petroleum*. 2020;6(1):1–13.
2 Morita N, Boyd PA. *Typical Sand Production Problems Case Studies and Strategies for Sand Control*. SPE; 1991.
3 Rahmati H, Jafarpour M, Azadbakht S, et al. Review of sand production prediction models. *J Petrol Eng*. 2013. https://doi.org/10.1155/2013/864981.
4 Volonté G, Francesco S, Brignoli M. Sand prediction: a practical finite-element 3D approach for real field applications. *SPE Prod Oper*. 2013;28(1):95–108.
5 Li X, Feng Y, Gray KE. A hydro-mechanical sand erosion model for sand production simulation. *J Petrol Sci Eng*. 2018;166:208–224.
6 Eshiet KII, Yang D, Sheng Y. Computational study of reservoir sand production mechanisms. *Geotech Res*. 2019;6(3):177–204.
7 Vardoulakis I, Stavropoulou M, Papanastasiou P. Hydro-mechanical aspects of the sand production problem. *Trans por med*. 1996;22(2):225–244.
8 Stavropoulou M, Papanastasiou P, Vardoulakis I. Coupled wellbore erosion and stability analysis. *Int J for Num An Meth Geomech*. 1998;22(9):749–769.
9 Gravanis E, Sarris E, Papanastasiou P. Hydro-mechanical erosion models for sand production. *Int J for Num An Meth Geomech*. 2015;18(39):2017–2036.
10 Wang H, Sharma MM. *A Fully 3-D, Multi-phase, Poro-Elasto-Plastic Model for Sand Production*. SPE; 2016.
11 Lu Y, Xue C, Liu T, et al. Predicting the critical drawdown pressure of sanding onset for perforated wells in ultra-deep reservoirs with high temperature and high pressure. *En Sci Eng*. 2021;9(9):1517–1529.
12 Honari S, Hosseininia SE. Particulate modeling of sand production using coupled DEM-LBM. *Energies*. 2021;14(4):906.
13 Papamichos E, Vardoulakis I, Tronvoll J, Skjaerstein A. Volumetric sand production model and experiment. *Int J for Num An Meth Geomech*. 2001;25(8):789–808.
14 Younessi A, Rasouli V, Wu B. Sand production simulation under true-triaxial stress conditions. *Int J Rock Mech Min Sci*. 2013;61:130–140.
15 Papamichos E. Analytical models for onset of sand production under isotropic and anisotropic stresses in laboratory tests. *Geomech Energy Env*. 2020;21, 100149.
16 Vardoulakis I, Sulem J. *Bifurcation Analysis in Geomechanics*. CRC Press; 1995.
17 Sinha BK, Papanastasiou P, Plona TJ. Influence of borehole over pressurization and plastic yielding on the borehole Stoneley and flexural dispersions. *J Geophys Res*. 1999;104(B7):15451–15459.
18 Sinha BK, Plona TJ. Wave propagation in rocks with elastic-plastic deformations. *Geophys Nor*. 2001;66(3):772–785.
19 Sarris E, Papaloizou L, Gravanis E. *A Hydro-Mechanical Constitutive Law for Modelling Sand Production*. ARMA; 2021, 21-1449.
20 Gravanis E, Sarris E, Papanastasiou P. *A Hydro-Mechanical Erosion Analytical Model for Sand Prediction*. ARMA; 2016, 16-335.
21 Fetrati M, Pak A. Numerical simulation of sanding using a coupled hydro-mechanical sand erosion model. *J Rock Mech Geotech Eng*. 2020;12(4):811–820.
22 Papamichos E, Stavropoulou M. An erosion-mechanical model for sand production rate prediction. *Int J Rock Mech Min Sci*. 1998;35(4):531–532.
23 Coussy O. *Poromechanics*. John Wiley & Sons; 2004.
24 Abaqus Abaqus. *Theory Guide*. USA: Dessault Systemes Simulia Corporation; 2020.
25 Shahsavari MH, Khamehchi E, Fattahpour V, Molladavoodi H. Investigation of sand production prediction shortcomings in terms of numerical uncertainties and experimental simplifications. *J Petrol Sci Eng*. 2021;207, 109147.